Vertical Cavity Surface-Emitting Laser Scanning Cytometer for High Speed Analysis of Cells*

P. L. Gourley and A. E. McDonald

Sandia National Laboratories
Albuquerque, NM 87185

M. F. Gourley

National Institutes of Health
Bethesda, MD 20892

ABSTRACT

We have constructed a new semiconductor laser device that may be useful in high speed characterization of cell morphology for diagnosis of disease. This laser device has critical advantages over conventional cell fluorescence detection methods since it provides intense, monochromatic, low- divergence light signals that are emitted from lasing modes confined by a cell. Further, the device integrates biological structures with semiconductor materials at the wafer level to reduce device size and simplify cell preparation. In this paper we discuss operational characteristics of the prototype cytometer and present preliminary data for blood cells and dielectric spheres.

1. INTRODUCTION

High speed analysis of dielectric particles is of interest for cellular diagnostics and environmental sensing. In this paper we discuss a prototype laser cytometer that has the potential to rapidly probe large populations of cells or dielectric particles. The cytometer is based on a biological microcavity laser technique[1] that employs a vertical cavity surface-emitting semiconductor to provide gain for light confined by cells. This laser technique has critical advantages over conventional fluorescence detection methods. The microcavity laser provides intense, monochromatic, narrow divergence light signals that are emitted from lasing modes confined by the cell. Once emitted from the microcavity, the light can be resolved into narrow spectral modes, high-contrast/coherent light images, or time-dependent pulses. These spectra, images, and time resolved data are useful for characterizing cell morphology and may be useful in diagnosis of cell abnormalities. We have used the cytometer in two basic configurations: first, as a probe of individual cells by spectral analysis of cell modes; second, as a scanning cytometer for rapidly probing large numbers of cells by pulse height spectroscopy.

A schematic of the instrument is shown in Fig. 1. A pump laser beam is directed through a pair of x-y scanning mirrors, through a dichroic beam splitter, and through an objective lens to the biocavity laser. The biocavity laser comprises cells or dielectric objects placed between a semiconductor wafer (with gain and mirror layers) and a top dielectric mirror. Light emitted normal to the biocavity mirrors is directed through the beamsplitter and a lens to a detector system, either solid state camera or a spectrometer/diode array

This work was supported by the United States Department of Energy under Contract DE-AC04-94AL85000.

detector combination. Thus, images and spectra of the emitted light can be obtained. In an alternate configuration, the output light is collected with a silicon avalanche photodiode to resolve laser pulses generated when the pump beam scans over a cell or sphere in the biocavity. In this configuration, output pulses can be collected by a pulse height analyzer for subsequent study.

We have used the first configuration to study spontaneous spectra of individual cells and dielectric spheres. These cells include red and white blood cells, and normal and malignant cells from tissues. We find that these cells have unique spectral signatures that can be used to identify them and determine their size and shape. Using the spectral separation of transverse modes, we have developed a method for sizing the cells and spheres. The validity of this method is supported by a theoretical model of the optical modes of a loaded Fabry-Perot resonator. The model is able to predict modal frequencies of differently shaped objects loading the resonator.

Using the alternate configuration, we have acquired pulse height spectra of single and multiple cells and spheres under low and high field of view conditions, respectively. In this case, the biocavity was operated well above the lasing threshold with high output intensity. To interpret these data, we have developed a simple model that relates scanning excitation of a single cell mode to the shape of a single cell pulse height spectrum. The experimental data are in qualitative agreement with this model which also provides a basis to interpret pulse height distribution of populations of cells.

2. INTRACAVITY LASER SPECTROSCOPY

Red and white blood cells, platelets, yeast cells and dielectric spheres have been studied by recording intracavity lasing spectra. We find that these cells have unique spectral signatures that can be used to identify them and determine their size and shape. We have previously discussed the details of the biocavity and how it can be operated above threshold to lase on single or multiple transverse modes established by the intracavity cell.[1] It is also possible to operate the laser below the lasing threshold to examine spontaneous spectra. In this case, all of the transverse modes of the cell-loaded cavity can be observed simultaneously. Since the spontaneous emission is relatively weak, a dominant longitudinal mode of the unloaded cavity is also present in the spectra. This provides a convenient reference line for measuring the wavelength shifts of the transverse cell modes. These shifts allow a precise determination of the refractive indices of the cells relative to the fluid surrounding them. The indices of the fluids are easily measured by refractometry. Thus, the absolute value of the cell indices can be accurately determined by this method. Further, the spectral separations of the transverse modes can be used to quantify the cell size.

A spectrum for the cavity loaded with a 6 micron sphere in water is shown in Fig. 2. Spectra for red and white blood cells in whole blood plasma diluted with saline are shown in Fig. 3. Also shown in these figures are reference spectra recorded in the bare cavity condition, where fluid is present, but no cell or sphere. The reference spectra differ due to changes in the fluid, cavity length, and wafers used. The spectral changes from the bare cavity to the cell-loaded cavity are evident as additional modal peaks near 850 nm. The number of modes, their spacings, intensity distribution, and red shifts from the bare cavity mode are distinctive for the sphere and each cell type. The average spacings of transverse modes (open points) are plotted against cell diameters in Fig. 4. These data are well described by simple 2-dimensional mode theory indicated by the solid line labeled B/d^2 where B is a constant and d is the cell diameter. This dependence is contrasted with the mode spacings observed for polystyrene spheres, also plotted in Fig. 4. In those data (solid points), the modes are

well described by a three-dimensional mode spacing indicated by the solid line labeled A/d. These data indicate that the spectra are sensitive to 3-dimensional cell/sphere shape as well as size.

3. INTRACAVITY LASER SCANNING CYTOMETER

In the second configuration of Fig.1, the device is operated as an intracavity scanning cytometer to probe many cells placed within a Fabry-Perot cavity defined by a vertical cavity surface-emitting laser wafer and a dielectric mirror. A scanning pump laser excites electron-hole pairs in the quantum wells in the semiconductor to create gain. A cell loaded in the cavity acts as dielectric waveguide to confine light and lower the laser threshold. When the scanning spot passes over the cell, as illustrated in Fig. 5, an intense pulse of laser light is emitted from the cavity. Since the cavity lifetime is the order of 10 picoseconds, the light pulse can be very short. Thus, many cells can be probed in a short period of time with high signal-to-noise light intensity. Using this principle, we have accumulated pulse height spectra of cell and dielectric sphere populations within a few seconds to minutes. Images and pulse height spectra for populations of polystyrene spheres and blood cells are shown in Figs. 6 and 7, respectively. These spectra exhibit distinctive peaks that reflect the cell/sphere size and uniformity in the populations.

3.1 Raster scan and cell sampling

In this and following sections, the operation of the scanning cytometer is discussed, including the effects of the scanning raster, wafer excitation, and light detection methods. The raster scan, illustrated in Fig. 5, has horizontal and vertical frequencies, f_x and f_y, respectively. The horizontal speed of the laser spot is $v_x=f_xA_x$ where A_x is the horizontal scan amplitude in the object plane. Likewise the vertical speed is $v_y=f_yA_y$ where A_y is the vertical scan amplitude in the object plane. The vertical separation of same direction scan lines is $s=f_yA_y/f_x$. The separation s can be adjusted relative to the cell size D. If the $s>>D$, the cell is unlikely to be sampled. If $s<<D$, the cell is sampled many times and the cell structure can be measured. However, few cells can be studied since data collection for a large number of cells consumes more time. For simply counting the cells, a good choice is the Nyquist sampling condition $s\approx D$ where each cell is sampled at least twice.

3.2 Laser pulse frequency

A pulsed laser excitation source is useful for pumping the laser cavity. The laser frequency f_o and pulse width t_p influence the horizontal sampling of the cell. The horizontal scan length during the laser pulse is $\ell=v_xt_p$ and the spacing between pulses $L=v_x/f_o$. To ensure satisfaction of the Nyquist condition in horizontal sampling, $L=D/2$. Combining x and y sampling conditions, we obtain a condition on the laser pulse frequency $f_o=(f_x^2/f_y)(A_x/A_y)$. If the amplitude ratio is set to 5:4 for a standard TV monitor, and a 4kHz resonant scanner is used in 1000:1 frequency ratio, we obtain f_o= 5 MHZ. Thus, high pulse frequencies are required. In most of the experiments described here f_0=4MHz.

3.3 Scan amplitude and Laser Spot Size

There is a compromise between the scanning field of view and the spot size. For small angles, the amplitude in the object plane is $A=F\theta$ where F is the objective focal length and θ is the angle of the scan

subtended by the objective. The laser spot size is $\delta=F\lambda/d$ where λ is the wavelength of the laser light and d is the beam diameter. Thus, the field of view and the spot size scale together. Typical values for the sampling parameters discussed above are summarized in table I.

TABLE I. RASTER SCAN PARAMETERS

field/spot conditions	scanning parameters for D=10μm cell size, f_o=4 MHZ, t_p=12 ns						
F (mm)/δ(μm)	f_x (Hz)	A_x (mm)	v_x (m/s)	s (μm)	L(μm)	ℓ(μm)	
	f_y (Hz)	A_y (mm)	v_y (mm/s)				
Small field 10/2	4000	0.25	1	0.2	0.25	0.012	
	4	0.20	0.8				
Large field 80/16	4000	5	20	4	5	0.24	
	4	4	16				

3.3 Excitation of optical modes in the biocavity

In the simplest analysis, the cross section of an optical mode in the wafer plane is a Bessel function of form $J_m(\alpha r)e^{im\theta}$ where $\alpha=2x_{mn}/D$ is the transverse wavevector, x_{mn} is the zero of the Bessel function, and m is the mode index. The excitation spot is approximately Gaussian of form $P(r)=\exp(-\beta r^2)$ with full width at half maximum (spot size) $\Delta=2\sqrt{\ln 2/\beta}$. The modal excitation and pulse output intensity is proportional to the overlap integral $I=2\pi\int_o^\infty \exp(-\beta r^2)J_m(\alpha r)rdr$. For the fundamental mode m=0 this can be evaluated directly as $I=2\pi\exp(-\alpha^2/4\beta)/2\beta$. This can be rewritten as $I=(a\pi\Delta^2/2)\exp(-ax_{00}^2\Delta^2/D^2)$ where a=1/4ln2. The maximum value of this function occurs at $\Delta_m=0.69D$. Thus, the optimum excitation of the fundamental mode occurs when the spot size is about 70% of the cell diameter. This is in close agreement with experiments where the spot size was adjusted with a prefocus lens to achieve optimal output intensity. Note that the spot size for optimal intensity is close to the line scan separation required for the Nyquist condition.

3.4 Output pulse detection

The pulses emitted by the biocavity are detected by a silicon photodiode, either a fast pin structure or an avalanche type having response times of several ns. In the experiments presented here, the excitation laser pulse width was 12 ns. The biocavity response time is ~10 ps so it can easily follow the excitation pulse. Thus, the biocavity output pulse is 12 ns. The output pulses are passed through a pulse-shaping amplifier with time constant of 1-3 μs and into a 200 MHZ Wilkinson-type multichannel analyzer with 512 channels. The conversion time for the analyzer is 2.5 μs per channel, slightly longer than the amplifier time constant. Thus, the upper limit on the cell detection rate is about 200 Khz. Note that the intrinsic sampling rate of the

biocavity is about 2 orders of magnitude higher than the detector and about five orders higher than the electronic converter. Even with faster electronics, the upper limit is the laser pulse frequency, in this case 4 MHZ.

Since the laser frequency is 4 MHZ, the 12 ns output pulses are separated in time by 250 ns. The transit time of the laser spot across the cell varies from 0.5 to 5 μs, depending on the horizontal velocity and cell size. Thus, anywhere from N=2 to 20 pulses per transit are obtained. The resulting pulse train will be integrated by the amplifier RC time constant, leaving only a single ~5 μs pulse per cell. The intensity of the integrated pulse S will be proportional to the number $N=Df_0/A_xf_x$ of excitation pulses during the transit. As a result, the pulse amplitude is proportional to the cell size.

In the pulse height spectra, the position of the peaks will be proportional to intensity, and the width of the peaks will be proportional to fluctuations in intensity. The fluctuations will depend on pump laser noise (usually less than 5%), mechanical vibrations in the optical hardware, and intracavity effects like cell motion and laser heating. Care must be taken to minimize all of these.

3.5 Single Cell Pulse Height Spectroscopy

The pulses can be accumulated in a multichannel analyzer to assess the distribution in pulse heights. The pulse height spectrum will be influenced by the variety of cell sizes and shapes. To understand how this is effected, we first consider the pulse height spectrum from a single cell sampled by a raster scan with horizontal line spacing s much less than the cell diameter. During successive line scans, the intersection of scan line and cell can range from near miss to direct hit. At different times, the line will be offset by R(t) from the cell center, and the pulse amplitude will be $I=2\pi\int_0^\infty \exp(-\beta(r-R)^2)J_m(\alpha r)rdr$. To first order, $I\sim\exp(-\beta R^2(t))$. Thus, successive scans will give a pulse train with a Gaussian envelope. Within this train, the probability of a given pulse height h is $P(h)=K\int dt\delta(I(t)-h)=K/|dI/dt|_{I=h}$ where K is a constant. For Gaussian pulses, P(h) has cusps at h=0 and $h=I_{max}$. Experimentally, these cusps will be rounded off by the finite resolution of the D/A converter. Consequently, the single cell spectrum will appear as a saddle-like function with peaks near h=0 and $h=I_{max}$.

Experimental data for a sphere and a red blood cell are shown in Figs. 6a and 7a, respectively. The spectrum for the sphere corresponds closely to a saddle-shaped curve with cusp-like features near the minimum and maximum values of the pulse heights. This is consistent with the Gaussian shape of the pulse train envelope shown by the upper right inset oscilloscope trace in Fig. 6a. In contrast, the spectrum for a red blood cell in Fig. 7a reveals a double-peaked structure at high pulse intensity and a monotonically decreasing tail to lower intensities. The photo inset of 7a clarifies these differences: the pulse train envelope is far from Gaussian. In contrast to the Gaussian envelope of 6a, the envelope of 7a is not symmetric, has more structure, and the tails are truncated. This pulse envelope is typical of the red blood cells. The cells are less symmetric than spheres and exhibit more internal structure. All of these differences are reflected in the pulse height spectra shown in Fig. 7a.

3.6. Multicell/sphere Pulse Height Spectroscopy

If many randomly distributed, identical cells are sampled with raster where s~D, the pulse height spectrum will be identical (aside from a multiplying factor) to the single cell spectrum. This is so because there is no correlation between the scan pattern and the relative position of the cells. All values of the offset R

between the scan line and cell center are equally probable. If the cell positions are correlated with the scan pattern, the spectrum will be enhanced or suppressed at certain pulse heights. However, this situation is not likely to occur.

The most common case occurs when the cells are randomly distributed and are not identical. When a population of such cells is examined, the pulse output will vary from cell to cell. These variations are of interest for assessing the characteristics of the population. The overall shape, positions and peak modulation are indicative of the variations in the cell population. Here, we expect the pulse height spectrum to be a composite of distinct single cell spectra. The cells will vary in size, shape, and internal structure giving rise to distinctive saddle-like spectra for each different cell type. Larger cells and cells with low internal scattering, will have a cusp/peak at higher pulse heights. Small cells and cells with high lasing thresholds will produce a cusp/peak shifted to lower pulse heights. All of the cells will produce a cusp/peak near h=0. Consequently, the composite spectrum will be very strongly peaked near h=0 and will have other distinct peaks at higher pulse heights. The number of these peaks will depend on the number of distinct cell types that dominate the distribution. If there exists a continuous variation in the cell characteristics, we expect the distinct peaks to be smeared over a continuous range of pulse heights.

Experimental spectra for multicell and multisphere scans are recorded in Figs. 6b and 7b, respectively. These spectra represent pulse heights for about a hundred spheres or cells. The spectrum for the spheres exhibits about seven distinct peaks that have widths comparable to the single sphere spectrum of Fig. 6a. A dominant peak exists near pulse height value of 3. Generally, the spectrum falls with increasing pulse height. Contrasting this spectrum, the red blood cell spectrum is nearly an exponentially decreasing function of pulse height with very slight peaks at selected pulse heights. These data indicate a much larger variation of cell size.

The spectra presented in Figs. 6 and 7 demonstrate that distinctive pulse height features for cells and spheres can be obtained simply by scanning a laser spot across the cell or sphere in the biocavity and integrating the output intensity over wavelength and cell transit time. The multicell and multisphere spectra are markedly different from their corresponding single cell or sphere spectra both in overall shape and detailed features. The observed differences in the single and multicell/sphere spectra are consistent with predictions by a simple analysis presented here.

4. CONCLUSIONS

We have presented novel methods for characterizing biological cells and small dielectric particles using semiconductor surface-emitting laser technology. One of the methods uses spontaneous emission of light confined by the cell or particle to define transverse spectral modes. The modal positions and spacing are sensitive to size and refractive index. Another method uses a scanning laser spot to excite lasing modes in the cells or particles to produce pulse height spectra that are sensitive to variations in cell/particle size and internal structure. These data demonstrate the feasibility of intracavity laser spectroscopy and scanning pulse height spectroscopy to assess characteristics of cells and dielectric particles. Future work should focus on improving time response, incorporating wavelength resolution in the scanning method, calibrating the instruments with standard specimens, and comparing the techniques with other standard methods.

5. REFERENCES

1. P. L. Gourley, K. E. Meissner, T. M. Brennan, B. E. Hammons, and M. F. Gourley, *Proceedings of the International Symposium on Biomedical Optics*, San Jose Feb. 4-10, 1995, SPIE vol. 2387, p 148.

ACKNOWLEDGEMENTS

We thank G. C. Loney and R. Zelany of General Scanning for supplying us with a mirror scanning apparatus, K. E. Meissner of Biotronics for collaborations on polystyrene sphere sizing, T. M. Brennan and B. E. Hammons for supplying semiconductor wafers, and A. E. Bieber for proofreading the manuscript. *This work was sponsored by the United States Department of Energy under contract DE-AC094AL85000, and supported in part by the Division of Materials Science, Office of Basic Energy Science. G1

Figure captions

Fig. 1. Schematic of the intracavity laser device showing a pump beam scanning over the biological microcavity laser (biocavity laser) resonator that is emitting a lasing beam toward a detector/spectrometer.

Fig. 3 Spontaneous emission spectra of the bare cavity, cavity loaded with 6 micron polystyrene spheres. The longitudinal modes of the bare cavity and the transverse modes of the cavity loaded with a sphere are indicated with vertical lines.

Fig. 2 Spontaneous emission spectra of the bare cavity, cavity loaded with a red blood cell, and loaded with a white blood cell, respectively. The longitudinal modes of the bare cavity are labeled with arrows. The transverse modes of the cavity loaded with a cell are indicated with vertical lines.

Fig. 4. Average transverse mode spacings as a function of measured cell diameter. Red and white blood cells and yeast cells are indicated with open points. These data are well described by the solid theoretical line labeled B/d^2 where B is a constant and d is the diameter. The mode spacings for polystyrene spheres (solid points) are also shown. These data are described by the theoretical line labeled A/d.

Fig. 5. Diagram illustrating the raster scan parameters.

Fig. 6. (a) Pulse height spectrum of a single 6 micron sphere. The inset photo shows the corresponding oscilloscope trace of the pulse train. (b) Pulse height spectrum of a distribution of ~100 spheres.

Fig. 7. (a) Pulse height spectrum of a single red blood cell. The inset photo shows the corresponding oscilloscope trace of the pulse train. (b) Pulse height spectrum of a distribution of ~100 red blood cells.

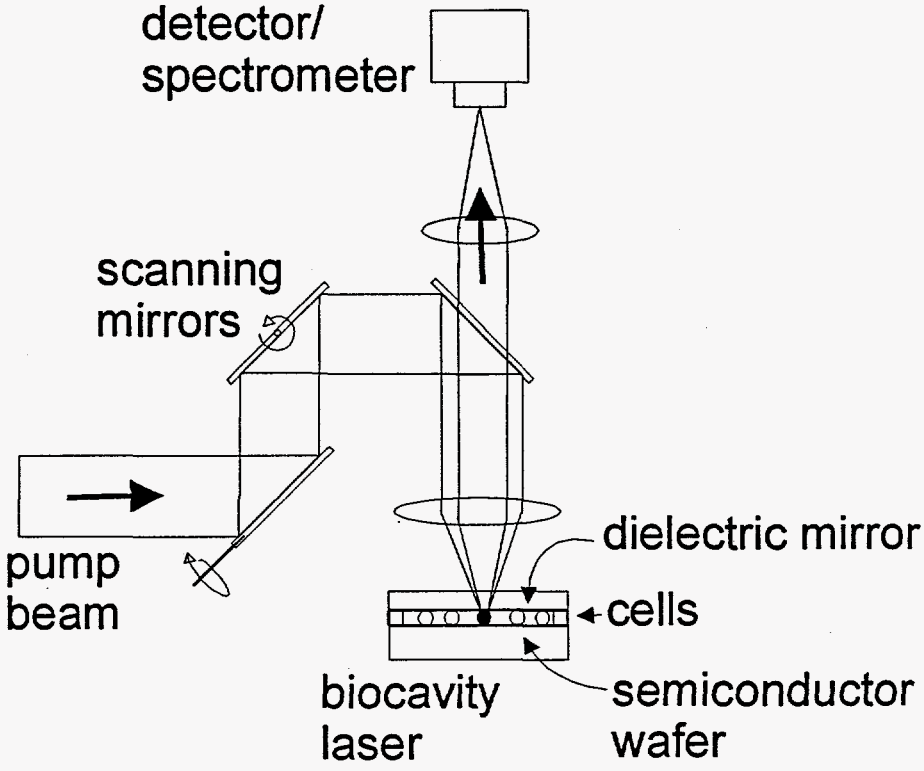
detector/
spectrometer
scanning
mirrors
pump
beam
dielectric mirror
cells
biocavity
laser
semiconductor
wafer

FIG. 1

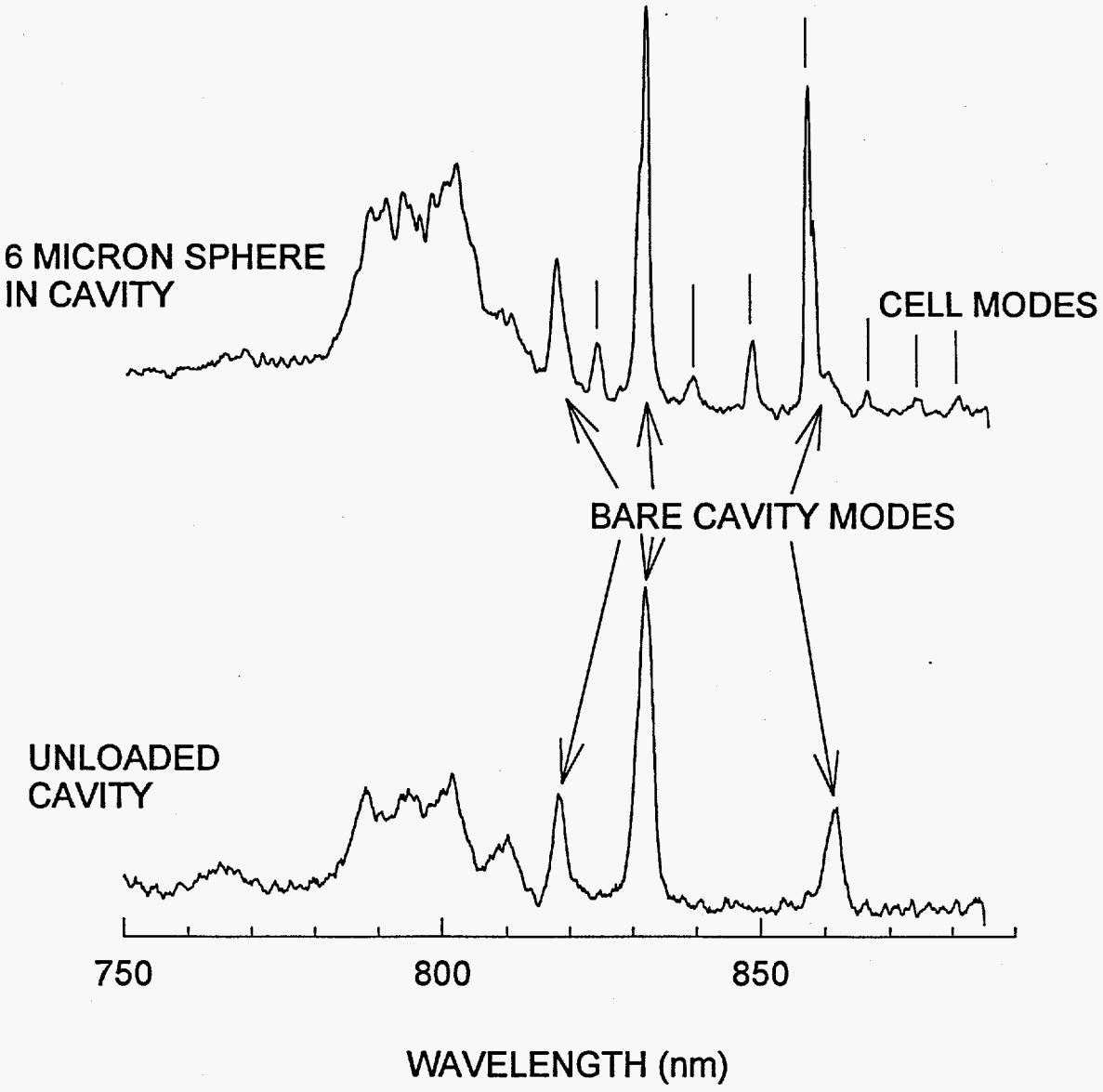
6 MICRON SPHERE
IN CAVITY
CELL MODES
BARE CAVITY MODES
UNLOADED
CAVITY
750
800
850
WAVELENGTH (nm)

FIG. 2

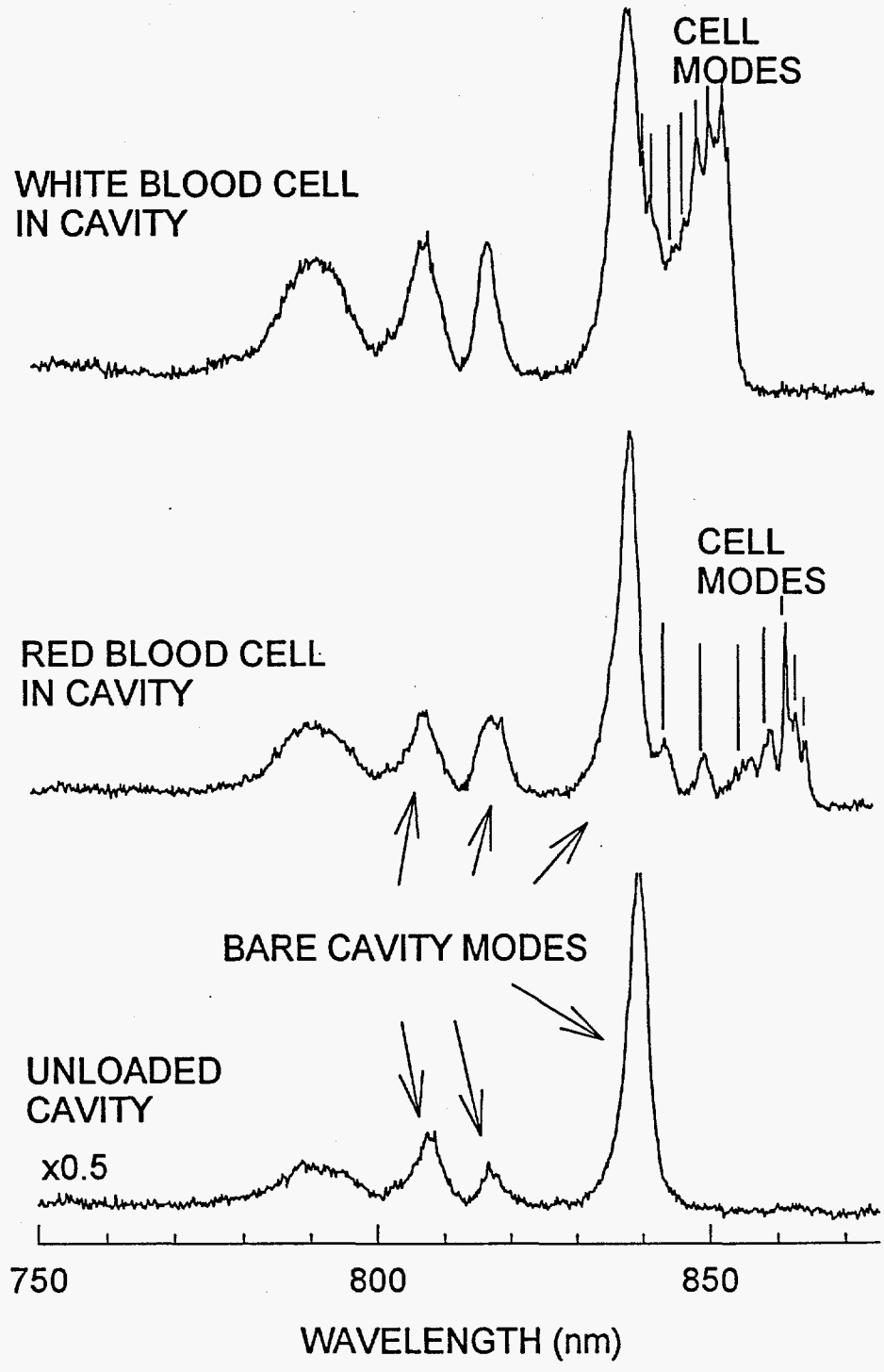
CELL
MODES
WHITE BLOOD CELL
IN CAVITY
CELL
MODES
RED BLOOD CELL
IN CAVITY
BARE CAVITY MODES
UNLOADED
CAVITY
x0.5
750
800
850
WAVELENGTH (nm)

FIG. 3

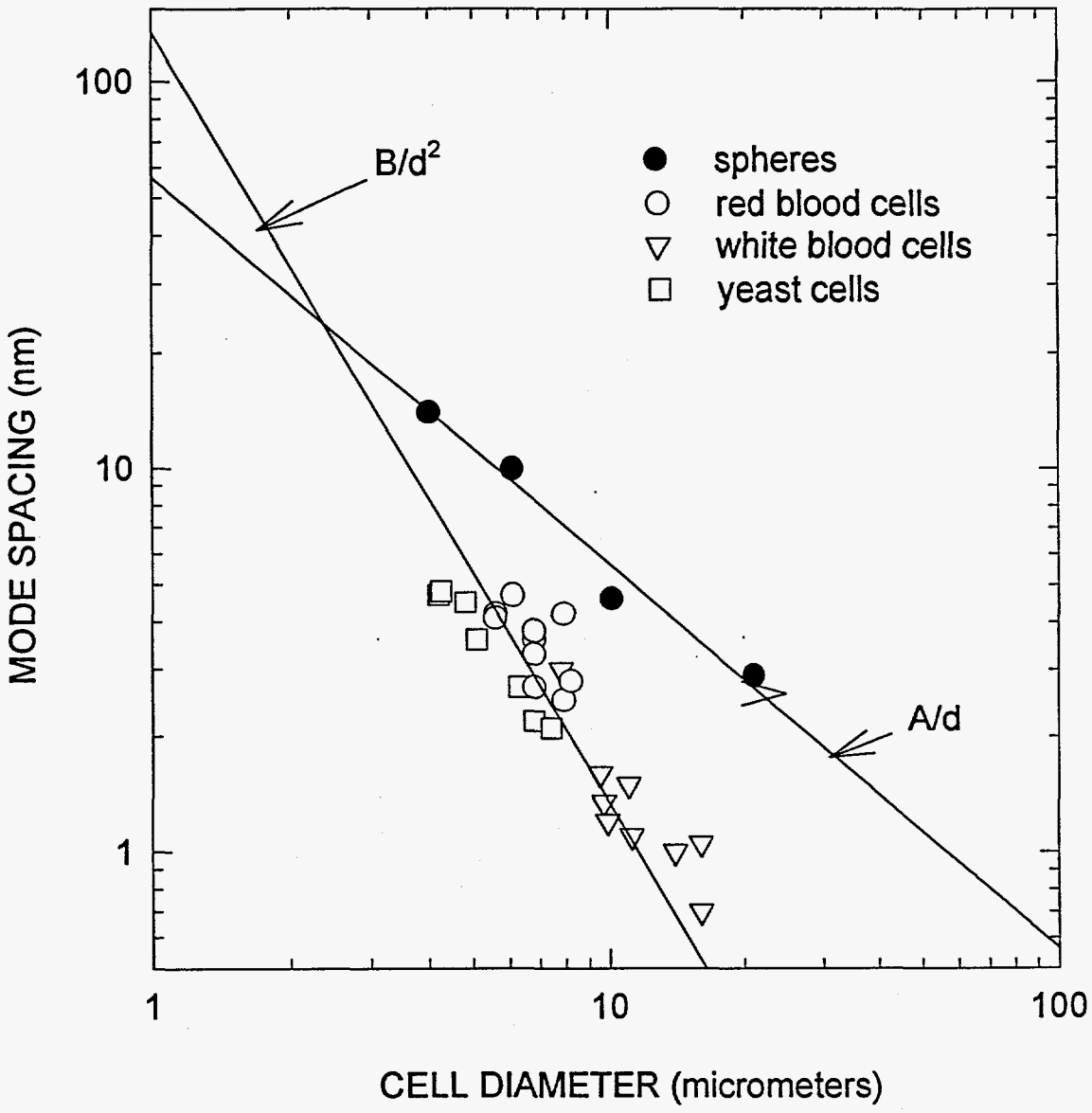
100
10
1
MODE SPACING (nm)
B/d²
A/d
spheres
red blood cells
white blood cells
yeast cells
1
10
100
CELL DIAMETER (micrometers)

FIG. 4

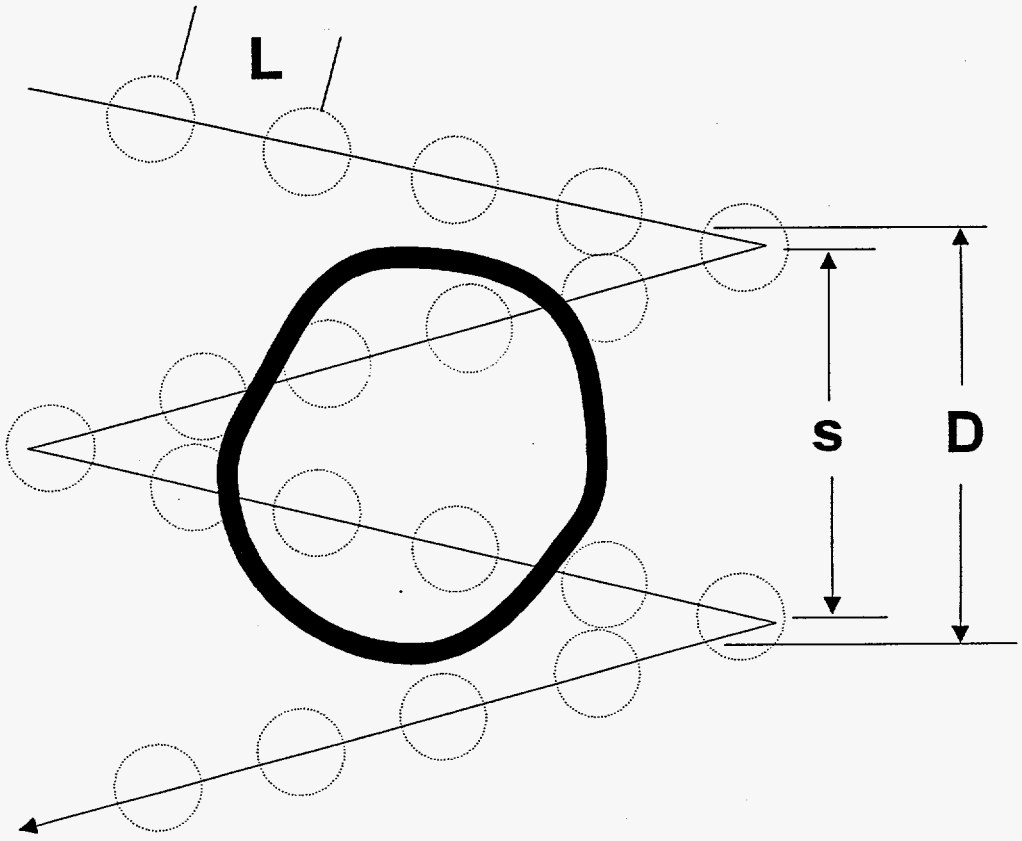

FIG. 5

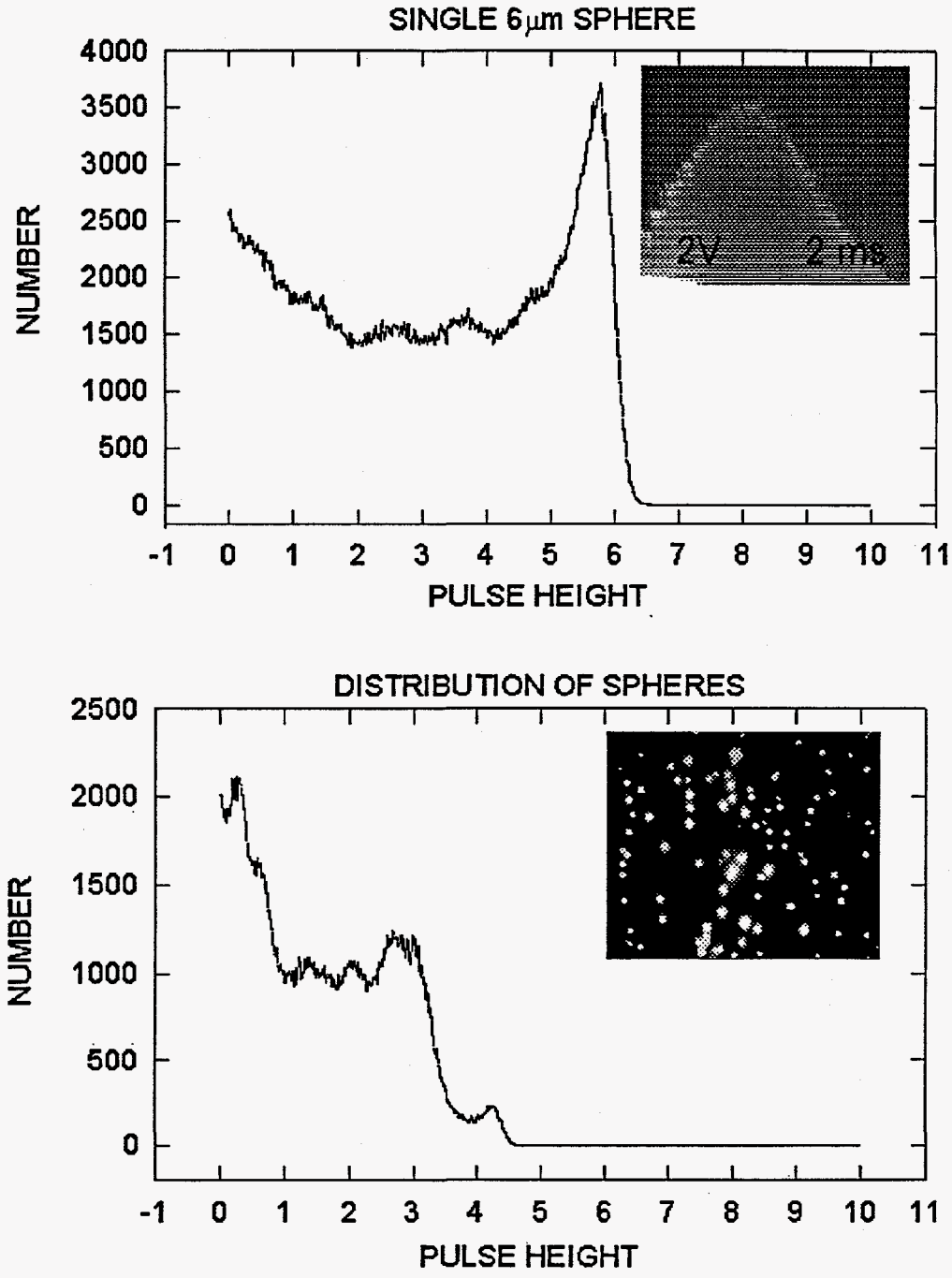
SINGLE 6μm SPHERE
NUMBER
4000
3500
3000
2500
2000
1500
1000
500
0
-1 0 1 2 3 4 5 6 7 8 9 10 11
PULSE HEIGHT
2V
2 ms
DISTRIBUTION OF SPHERES
NUMBER
2500
2000
1500
1000
500
0
-1 0 1 2 3 4 5 6 7 8 9 10 11
PULSE HEIGHT

FIG. 6

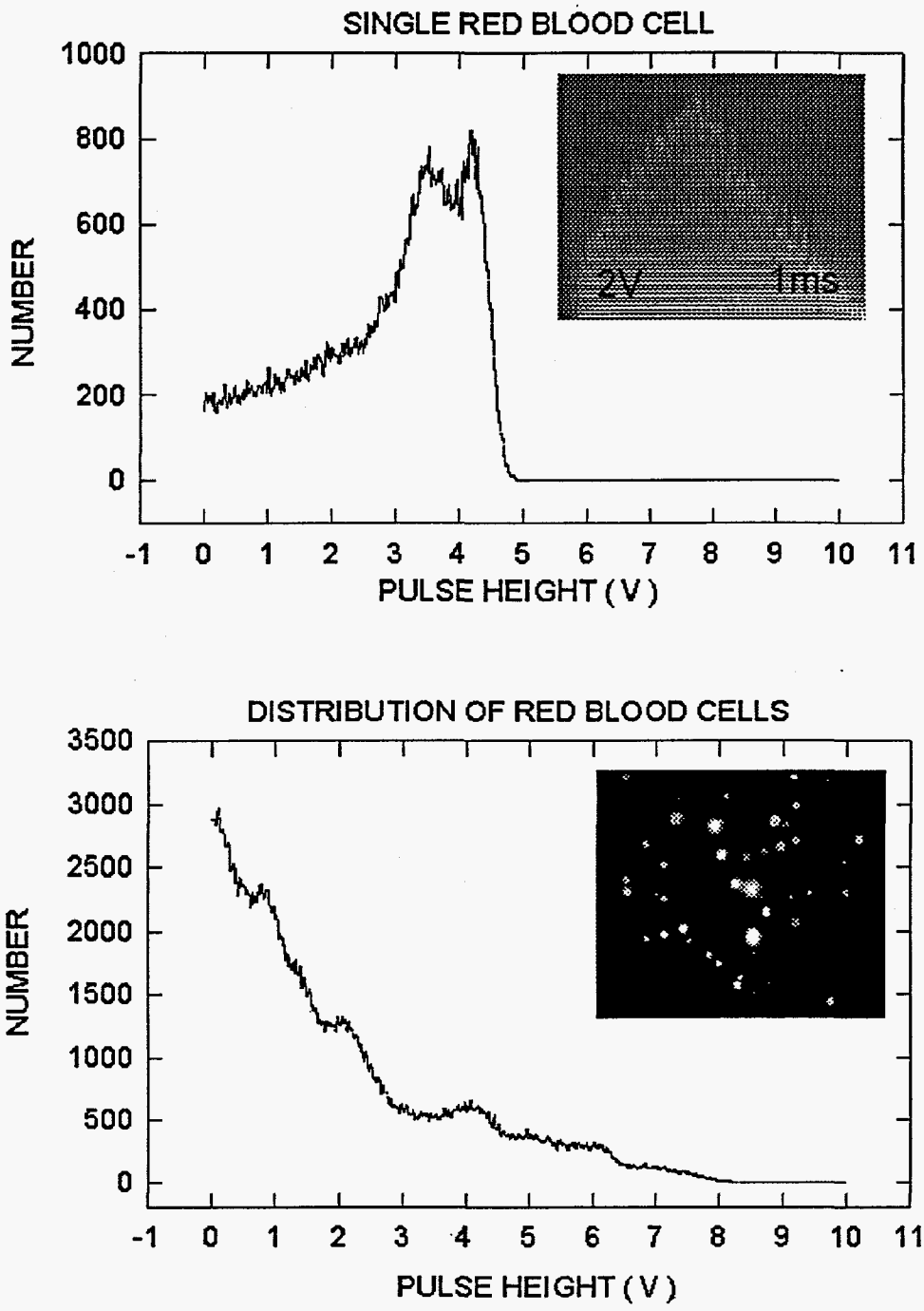
SINGLE RED BLOOD CELL
NUMBER
1000
800
600
400
200
0
-1 0 1 2 3 4 5 6 7 8 9 10 11
PULSE HEIGHT (V)
2V
1ms
DISTRIBUTION OF RED BLOOD CELLS
NUMBER
3500
3000
2500
2000
1500
1000
500
0
-1 0 1 2 3 4 5 6 7 8 9 10 11
PULSE HEIGHT (V)

FIG. 7